

Simulations of Runaway Electron Generation including Hot-Tail Effect

H. Nuga¹, M. Yagi² and A. Fukuyama¹

¹Kyoto University, Kyoto, Japan

²National Institute for Quantum Radiological Science and Technology, Aomori, Japan

Corresponding Author: nuga@p-grp.nucleng.kyoto-u.ac.jp

Abstract:

The suppression and mitigation of runaway electron (RE) in disruptions are urgent issues of large scale tokamak operation. The contribution of hot-tail effect, which arises from fast thermal quench, is studied using two-dimensional Fokker-Planck simulation. It is found that if the thermal quench is fast enough to invoke the hot-tail effect, it might produce seed REs and enhance total RE current even in a high electron density plasma ($n_e \sim 10^{21} \text{ m}^{-3}$) achieved by massive gas injection (MGI).

1 Introduction

Disruption is one of the most serious events in tokamaks, since it induces huge electromagnetic force to the device and generates high-energy REs which may cause the damage of plasma facing components[1]. In ITER, the RE current is considered to reach a few mega-amperes. To avoid the disruption and related damages, fast plasma shutdown by using MGI has been proposed. It is expected that owing to the high collisionality, the high electron density plasma achieved by MGI may suppress the RE generation. However, MGI for mitigating disruption shortens the thermal quench duration, and may enhance the primary RE generation rate through the so-called “hot-tail effect[2, 3]”.

To describe RE generation processes including the hot-tail effect and predict the disruption dynamics in ITER, kinetic Fokker-Planck simulation of electron distribution function is required. In the present analysis, the primary RE generation rate is evaluated by the electron momentum distribution function obtained by using two-dimensional Fokker-Planck equation. Evolutions of RE generation and induced electric field is calculated self-consistently[4, 5, 6].

2 Basic equations

In this section, the induced toroidal electric field, the primary and secondary RE generation rates, the thermal quench of bulk plasma, and the increase of electron and ion

densities and the effective charge are modeled.

The primary RE generation rate is defined from the relativistic momentum distribution function, which obeys the Fokker-Planck equation:

$$\frac{\partial f}{\partial t} = -\nabla \cdot \left[-\overleftrightarrow{\mathbf{D}}_C \cdot \nabla f + \left(\mathbf{F}_C + \frac{q\mathbf{E}}{m_e} \right) f \right], \quad (1)$$

where ∇ is the derivative operator in momentum space (p, θ). They denote the momentum and the pitch angle, respectively. The collisional diffusion and friction terms, $\overleftrightarrow{\mathbf{D}}_C$ and \mathbf{F}_C , are determined the weak relativistic isotropic background collision term[7, 8] with relativistic Maxwellian.

2.1 Electric field and RE generation rate

The induced toroidal electric field E obeys the following equations[5, 6]:

$$\frac{1}{r} \frac{\partial}{\partial r} \left(r \frac{\partial E}{\partial r} \right) = \mu_0 \frac{\partial j}{\partial t}, \quad (2)$$

$$j = \sigma_{\parallel} E + ecn_r, \quad (3)$$

$$\frac{dn_{rp}}{dt} = \int \nabla \cdot \mathbf{S}_{C,E} d\mathbf{p}, \quad (4)$$

$$\frac{dn_{rs}}{dt} = S_{avalanche}(n_r, E/E_C), \quad (5)$$

where $E_C = n_e q_e^3 \ln \Lambda / 4\pi \varepsilon_0^2 m_e c^2$. The boundary condition for the electric field is obtained by the expression of E in vacuum region: $E(r) \propto \ln(r/b)$, where $r = b$ is the location of the wall. σ_{\parallel} in eq. (3) is the Spitzer conductivity $\sigma_{sp} = 1.96 n_e q_e^2 \tau_e / m_e$ with neo-classical correction[9], where $\tau_e = 3(2\pi)^{3/2} \varepsilon_0^2 m_e^{1/2} T_e^{3/2} / Z_{\text{eff}} n_e q_e^4 \ln \Lambda$. The total RE density n_r is given by $n_r = n_{rp} + n_{rs}$, where n_{rp} and n_{rs} are the primary and secondary RE densities, respectively. For simplicity, we adopt the cylindrical geometry for the calculation of the electric field. The Ohm's law (eq. (3)) provides a closure for the diffusion equation of the toroidal electric field (eq. (2)). Here, we split the plasma current into two components: the ohmic current $\sigma_{sp} E$ and RE current ecn_r . It is assumed that all of REs travel with the velocity of light.

The two kind of RE densities are obtained by eqs. (4) and (5). The primary RE generation rate is determined by calculating the flux through the boundary of momentum calculation domain: $0 < p < p_{\text{max}}$. This means that the electrons whose momentum is greater than p_{max} are regarded to be REs. In the present paper, we choose the upper boundary as follow: $(p_{\text{max}})^2 / (2m_e) \sim 0.5 \text{ MeV}$. This is because we focus on not RE distribution in high energy region (\sim tens of MeV) but the number of REs generated in disruptions. The validity of the choice of p_{max} was discussed in Ref. [6]. Contrary to the primary RE generation rate, the secondary RE generation rate is given by a function[10] of n_r and E/E_C rather than the momentum distribution. This is because the secondary RE generation rate is insensitive to the primary RE energy[11].

2.2 Thermal quench and MGI

In order to simulate RE generation in disruptions, a simple model for the thermal quench is adopted. Although the behavior of the plasma temperature during thermal quench is very complex, here, the decay of the background plasma temperature is given by a simple model:

$$T(t, \rho) = (T_0(\rho) - T_f(\rho)) \exp(-t/\tau_q) + T_f(\rho), \quad (6)$$

$$T_0(\rho) = (T_0(0) - T_0(1))(1 - \rho^2)^2 + T_0(1), \quad (7)$$

$$T_f(\rho) = T_f(0)(1 - 0.9\rho^2), \quad (8)$$

where ρ is the normalized minor radius, τ_q denotes the time constant of the thermal quench, and T_0 and T_f are the pre- and post-quench plasma temperature. Here ions and electrons are assumed to have the same temperature. Here ions and electrons are assumed to have the same temperature. The collision terms \mathbf{D}_C and \mathbf{F}_C with decaying background temperature deform the momentum distribution function of pre-quench temperature to that of post-quench temperature by solving eq. (1). Although the behavior of the plasma temperature during thermal quench is very complex, here, the decay of the background plasma temperature is simplified.

The evolutions of electron and ions densities and the effective charge assuming MGI are modeled. Usually, noble gas, such as neon or argon, is used for MGI. In the low temperature plasma (\sim tens of eV), however, most of impurity ions are not fully ionized. Since the issue of ionization state of impurities is complex, to simplify our model, we introduce post-MGI effective charge Z_{eff}^f and hypothetical impurity ion species, which has no binding electron. Additionally, the influence of the presence of the binding electron to the conductivity is also omitted. They satisfy the following relations:

$$n_e^f = n_e^0 + Z_i n_i^f, \quad Z_{\text{eff}}^f = \frac{n_D + Z_i^2 n_i^f}{n_e^f}, \quad (9)$$

where, superscript 0 and f denote pre-quench and post-MGI density or effective charge and subscript e , D and i denote ion species (electron, deuteron and impurity ion), respectively. In the following calculation, n_e^0 , n_e^f , n_D , Z_{eff}^f are given, in contrary, n_i^f and Z_i are obtained to satisfy the relation. Similarly, evolution of the electron density is modeled as follows:

$$n_e^0(\rho) = (n_e^f(\rho) - n_e^0(\rho)) \frac{t}{\Delta t_{\text{MGI}}} + n_e^0(\rho) \quad (0 < t < \Delta t_{\text{MGI}}) \quad (10)$$

$$n_e^0(\rho) = n_e^f(\rho) \quad (\Delta t_{\text{MGI}} < t), \quad (11)$$

where Δt_{MGI} is the duration in which electron density increases. Although impurities are transported from outer region in fact, our model does not solve the radial transport and assumes to keep radial dependence of electron and ion densities for simplicity. The example of the evolution of the temperature and electron density are illustrated in Figure 1.

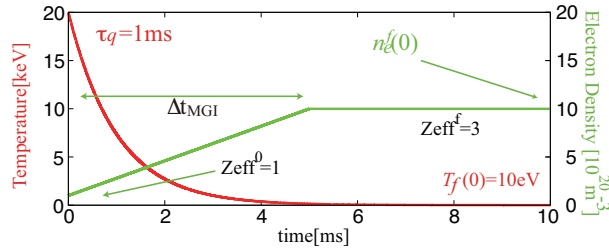


FIG. 1: Model of thermal quench and density increase.

3 Hot-tail effect with MGI

The high density plasma ($\sim 10^{21} \text{ m}^{-3}$) is desired to suppress the RE generation. Since the critical electric field E_C is proportional to the electron density, the secondary RE generation may be suppressed when the electric field is kept below the critical electric field E_C ($E/E_C < 1$). Moreover, even if $E/E_C > 1$, the high collisionality of the high density plasma may prevent from generating primary REs. If the hot-tail is formed, however, the less collisional hot-tail electron may produce primary REs. Therefore we examined the density dependence of the hot-tail effect. In the following calculation, we employ parameters tabulated in Table I.

TABLE I: PLASMA PARAMETERS

Radii	$R = 6.2\text{m}, a = 2.0\text{m}, b = 2.4\text{m}$
Initial current	15 MA
Current density	$j_0(1 - \rho^2)$
Initial temperature	$T_0(0) = 20 \text{ keV}, T_0(1) = 2 \text{ keV}$
Post-quench temp.	$T_f(0) = 10 \text{ eV}$
Initial Density profile	$n_e^0(\rho) = (n_e^0(0) - n_e^0(1))(1 - \rho^2)^{0.67} + n_e^0(1)$ $n_e^0(0) = 1.0 \times 10^{20} \text{ m}^{-3}$ $n_e^0(1) = 1.0 \times 10^{19} \text{ m}^{-3}$
Initial effective charge	$Z_{\text{eff}}^0 = 1$
Ion species	Deuteron

Additionally, in the following calculation, we employ the time constant of the thermal quench $\tau_q = 1 \text{ ms}$, the duration $\Delta t_{\text{MGI}} = 5 \text{ ms}$, and the post-MGI effective charge $Z_{\text{eff}}^f = 3$. If we do not consider the density increase, in our model, the ratio of τ_q and the electron-electron slowing down time for a few time of pre-quench thermal velocity $\tau_s^{ee}(2 - 3v_{\text{th0}})$ can be seen as a threshold value of the hot-tail effect[5, 6]. Namely, if the ratio satisfies $\tau_q/\tau_s^{ee}(3v_{\text{th0}}) > 1$, the hot-tail effect may be suppressed. The value $\tau_q = 1 \text{ ms}$ is sufficiently short to invoke the hot-tail effect for $n_e^f = 10^{20} \text{ m}^{-3}$ ($\tau_q/\tau_s^{ee}(3v_{\text{th0}}) \sim 0.26$). Contrary, for high density case ($n_e^f = 10^{21} \text{ m}^{-3}$), the ratio becomes greater than a unit ($\tau_q/\tau_s^{ee}(3v_{\text{th0}}) \sim$

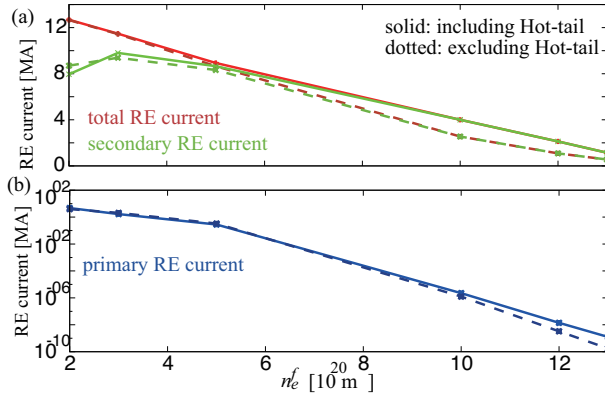


FIG. 2: $n_e^f(0)$ dependence of the total, primary, and secondary RE current for $\tau_q = 1$ ms, $\Delta t_{\text{MGI}} = 5$ ms, and $Z_{\text{eff}}^f = 3$.

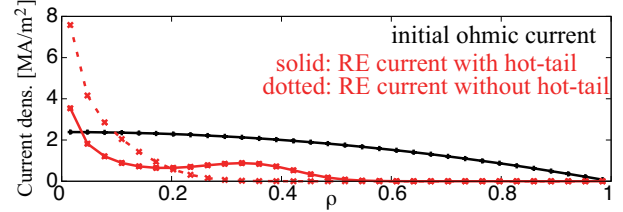


FIG. 3: Current density profile for $n_e^f(0) = 12 \times 10^{20} \text{ m}^{-3}$.

2.6). In the following calculation, however, electron density increases in time. Therefore the ratio do not always become the threshold value.

Figure 2 shows the $n_e^f(0)$ dependence of the (a) total, secondary, and (b) primary RE current. It is found that the density increase achieves to suppress the RE generation as expected. In low density region (ex. $n_e^f(0) = 2 \times 10^{20} \text{ m}^{-3}$), most of initial ohmic current is converted into RE current (total RE current: $I_{\text{RE}} = 12.7$ MA). On the other hand, in high density region ($n_e^f(0) = 1.2 \times 10^{21} \text{ m}^{-3}$), RE current is suppressed to a few Mega Amperes. Moreover, the suppression of the primary RE generation is remarkable. The ratio of the primary RE current to total RE current decreases with the increase of $n_e^f(0)$. Although, the high density succeeds to suppress the RE generation, the presence of the hot-tail effect makes the total RE current twice in $n_e^f(0) = 12 \times 10^{20} \text{ m}^{-3}$ case ($I_{\text{RE}} = 1.09$ and 2.12 MA for excluding and including hot-tail effect cases). Note that, in the excluding hot-tail case, RE generation rate model derived by Connor and Hastie[12] is used for the primary RE generation rate instead of eq. (4).

Subsequently, we focus on $n_e^f(0) = 12 \times 10^{20} \text{ m}^{-3}$ case in which the presence of the hot-tail effect doubles the total RE current. Figure 3 shows the initial ohmic and RE current density profiles. Nevertheless of the presence or absence of the hot-tail effect, the RE current density profiles have a peak on axis rather than the initial profile. Furthermore, the hot-tail effect makes the peak lower and broadens the RE current profile. Figures 4 show the evolutions of (a) total and RE current, (b) induced electric field on axis and (c) $\rho = 0.3$, and (d) primary and secondary RE generation rates on axis and (d) $\rho = 0.3$. From fig. 4 (d) and (e), it is found that the hot-tail effect makes a additional peak of the primary RE generation rate ($t \sim 5$ ms). This is because, hot-tail electrons can be REs easily rather than bulk electrons even with the weak electric field due to the low collisionality. Owing to the presence of earlier seed REs, the secondary RE generation is also triggered earlier. On $\rho = 0.3$, since the primary RE generation rate at first additional peak ($t \sim 5$ ms) is sufficiently greater than that at subsequent peak ($t \sim 10$ ms, originates from the bulk electron), the secondary RE current also becomes greater. On the other

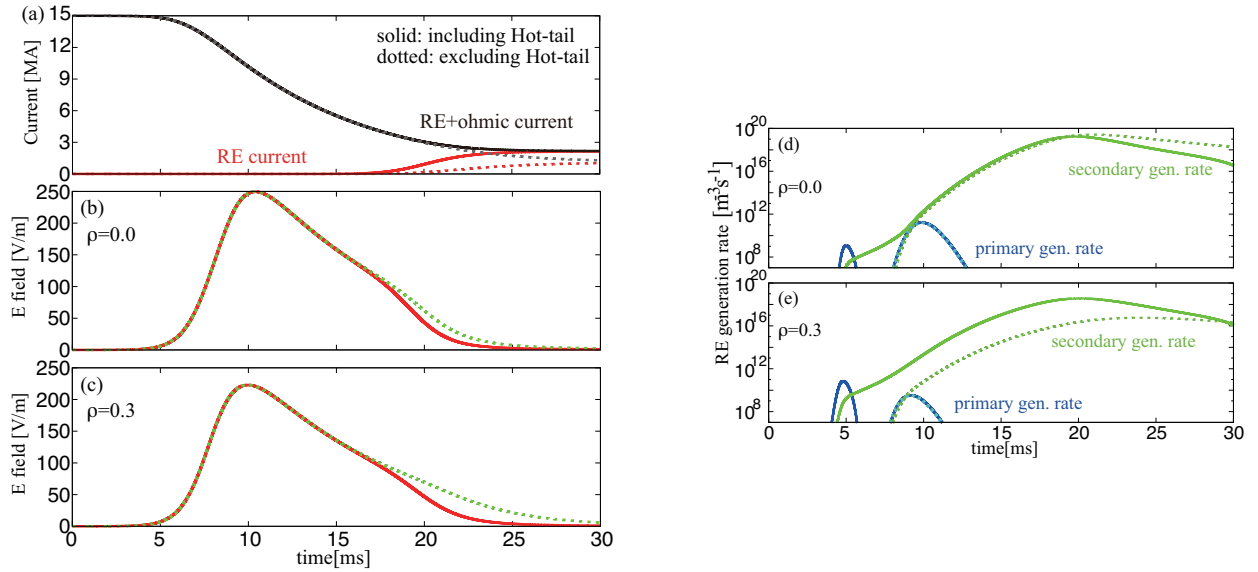


FIG. 4: Evolutions of (a): Total and RE current, (b,c): electric field on $\rho = 0$ and $\rho = 0.3$, and (d,e): primary and secondary RE generation rates.

hand, on axis, since the additional peak is sufficiently smaller than the subsequent one, the secondary RE generation is similar to that of excluding hot-tail case until $t \sim 20$ ms. Once RE current starts to generate, the induced electric field is reduced to conserve poloidal magnetic flux. From fig. 4-(c), it is found that the electric field becomes weaker than that of excluding hot-tail case after $t \sim 17$ ms. The reduction of the electric field on $\rho = 0.3$ decreases that on axis via electric diffusion (fig. 4-(b)). Since the reduction of electric field on axis affects the secondary RE generation, consequently, RE current density on axis decreases and its profile is broadened.

This result shows that the presence of the first additional peak of the primary RE generation ($t \sim 5$ ms) multiplies the total RE current. In the result, $\Delta t_{\text{MGI}} = 5$ ms is chosen. This means that the hot-tail RE start to be generated before the electron density reaches post-MGI density n_e^f . Therefore, next, $\Delta t_{\text{MGI}} = 3$ ms is chosen to investigate the behavior of the hot-tail RE peak. Figure 5 shows the primary RE generation rate for $\Delta t_{\text{MGI}} = 5$ ms and 3 ms cases. It is found that the faster increase of the electron density achieves to suppress the hot-tail RE generation ($t \sim 5$ ms) both on axis and $\rho = 0.3$. Consequently total RE current is also suppressed to 1.09 MA, which nearly equals to the result excluding hot-tail. Fast increase of n_e also reduces E/E_D as shown in Figure 6, where E_D is the Dreicer electric field. Since the primary RE generation is very sensitive to E/E_D , the reduction of E/E_D during hot-tail generation phase achieves to suppress the generation.

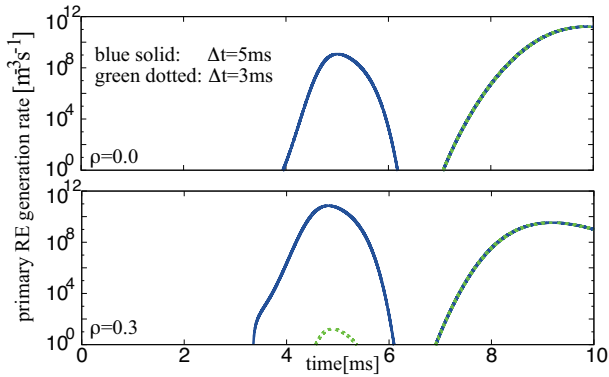


FIG. 5: Primary RE generation rate on axis and $\rho = 0.3$ for $\Delta t_{\text{MGI}} = 5$ ms and 3 ms.

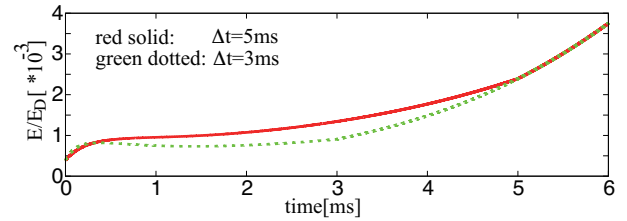


FIG. 6: Evolutions of E/E_D for $\Delta t_{\text{MGI}} = 5$ ms and 3 ms.

4 Conclusion

We have applied the kinetic Fokker-Planck simulation to describe the RE generation including the hot-tail effect in disruptions with MGI mitigation. We have confirmed that the RE generation is suppressed with the increase of the electron density. If the hot-tail effect is not considered, the RE generation is reduced to ~ 1 MA in the high density region ($n_e^f(0) = 12 \times 10^{20} \text{ m}^{-3}$). On the other hand, if the hot-tail effect is included, the effect doubles the RE current in the high density region. This multiplication comes from the fact that hot-tail electrons can be REs earlier than bulk electrons owing to its low collisionality. If the electron density increases up insufficiently until the hot-tail RE generation starts, the hot-tail effect multiplies the RE current. Conversely, it is also confirmed that sufficiently fast increase of the electron density may suppress the hot-tail RE generation.

The present simulation study makes clear that the hot-tail effect is important for the RE generation with short thermal quench even in high electron density plasma. There is a possibility that MGI planned for ITER operation to avoid the RE generation in disruptions shortens the thermal quench duration and invokes the hot-tail effect, which may produce non-negligible primary RE current and large secondary RE current. Conversely, if the increase of the electron density is sufficiently faster than hot-tail RE generation, MGI may suppress the hot-tail effect. In these phenomena, reliable estimation of the thermal quench, increase of the electron density, and impurity transport is inevitable.

References

- [1] T.C. Hender et al., Nucl. Fusion, **47**, S128 (2007)
- [2] H. Smith and E. Verwichte, Phys. Plasmas, **15**, 072502 (2008).
- [3] T. Fehér, H. Smith, T. Fülöp, et al, Plasma Phys. Conrol. Fusion, **53**, 035014 (2011).

- [4] H. Nuga, A. Matsuyama, M. Yagi, and A. Fukuyama, *Plasma Fusion Res.*, **10**, 1203006 (2015).
- [5] H. Nuga, A. Matsuyama, M. Yagi, and A. Fukuyama, *Plasma Fusion Res.*, **11**, 240323 (2016).
- [6] H. Nuga, M. Yagi, A. Fukuyama, *Phys. Plasmas*, **23**. 062506 (2016).
- [7] C. Karney, *Comput. Phys. Rep.* **4**, 183, (1986).
- [8] C.F.F. Karney and N.J. Fisch, *Phys. Fluids*, **28**, 116, (1985).
- [9] J. Wesson, *Tokamaks*, 3rd ed. (Oxford University Press, 1987)
- [10] M.N. Rosenbluth and S.V. Putvinski, *Nucl. Fusion*, **37**, 1355 (1997).
- [11] S. Chiu, M. Rosenbluth, and V. Chan, *Nucl. Fusion*, **38**, 1711 (1998).
- [12] J.W. Connor and R.J. Hastie, *Nucl. Fusion*, **15**, 415 (1975).